Journal of Environmental Management 238 (2019) 341–351

Contents lists available at ScienceDirect

Journal of Environmental Management

journal homepage: www.elsevier.com/locate/jenvman

Research article

Spatial Bayesian Network for predicting sea level rise induced coastal erosion in a small Pacific Island

Oz Sahin[a,b,c,*], Rodney A. Stewart[b,c], Gaelle Faivre[a,c], Dan Ware[a,c], Rodger Tomlinson[c], Brendan Mackey[a]

[a] Griffith Climate Change Response Program, Griffith University, QLD, Australia
[b] School of Engineering and Built Environment, Griffith University, QLD, Australia
[c] Griffith Centre for Coastal Management and Cities Research Institute, Griffith University, QLD, Australia

ARTICLE INFO

Keywords:
Spatial Bayesian Network
Probabilistic coastal hazard mapping
Climate change risk
Probabilistic risk mapping

ABSTRACT

An integrated approach combining Bayesian Network with GIS was developed for making a probabilistic prediction of sea level rise induced coastal erosion and assessing the implications of adaptation measures. The Bayesian Network integrates extensive qualitative and quantitative information into a single probabilistic model while GIS explicitly deals with spatial data for inputting, storing, analysing and mapping. The integration of the Bayesian Network with GIS using a cell-by-cell comparison technique (aka map algebra) provides a new tool to perform the probabilistic spatial analysis. The spatial Bayesian Network was utilised for predicting coastal erosion scenarios at the case study location of Tanna Island, Vanuatu in the South Pacific. Based on the Bayesian Network model, a rate of the island shoreline change was predicted probabilistically for each shoreline segment, which was transferred into GIS for visualisation purposes. The spatial distribution of shoreline change prediction results for various sea level rise scenarios was mapped. The outcomes of this work support risk-based adaptation planning and will be further developed to enable the incorporation of high resolution coastal process models, thereby supporting localised land use planning decisions.

1. Introduction

1.1. Coastal erosion hazard assessment

Anticipated sea level rise (SLR) on coastal regions is expected to exacerbate the impact of coastal hazards such as erosion, inundation, flooding from storm surge with increasing frequency and intensity, land loss, and saline intrusion. Consequently, the resulting impacts on coastal settlements and infrastructure will be widespread. These impacts are particularly crucial in small islands as the settlements and infrastructure are mainly located along the coastlines with almost no, or very limited relocation options (Nurse et al., 2014). As a result, some of the coastal zones of these small island states could become uninhabitable (Hewitson et al., 2014). Therefore, identification and assessments of coastal hazards are critical for planning and developing effective management strategies to protect lives and properties exposed to coastal hazards. Thus, effective management of these areas for reducing the potential impacts of coastal hazards is one of the most critical priorities for the governments and local communities in the region.

Erosion is the movement of sediments in response to waves, wind and sea levels. Erosion is a naturally occurring coastal process without which many coastal landforms in particular beaches would not exist. Erosion becomes problematic or a hazard when its interaction causes change or damage to assets of value such as the loss of land or damage to buildings, roads or other infrastructure. Erosion can be distinguished temporally from short-term responses to storm events, beach rotation where the alignment of shore shifts in response to seasonal changes in wind and waves and as recession a longer-term process where shorelines shift landward. The focus of this paper is on predicting, and planning for, rare or unprecedented coastal erosion events related to longer term climate change affects to coastal regions.

There are three main approaches for the assessment of coastal erosion hazards: (1) Erosion prone area (Shand et al., 2015); (2) Beach Volume Index (Todd et al., 2015); and (3) Vulnerability Index (Alexandrakis and Poulos, 2014). Each approach provides a different outcome which seeks to serve a different purpose. The erosion prone area is predictive and two dimensional; it breaks down a series of components, storm erosion, long-term recessions, sea level rise erosion and foundation instability, to quantify each into a width that can be used to inform land use planning and to establish building setbacks.

* Corresponding author. Griffith Climate Change Response Program, Griffith University, QLD, Australia.
E-mail address: o.sahin@griffith.edu.au (O. Sahin).

https://doi.org/10.1016/j.jenvman.2019.03.008
Received 21 November 2018; Received in revised form 20 February 2019; Accepted 2 March 2019
Available online 08 March 2019
0301-4797/

While this approach is the most readily applied in practice, the deterministic nature is at odds with the needs of a risk-based approach to identifying responses to coastal hazards.

The beach volume index is diagnostic and is distinct from the erosion prone area approach in that it takes a three-dimensional approach based on coastal process knowledge that the volume of sediment across the active beach is more important than the width in determining its erosion hazard. While this approach demonstrates a superior awareness of coastal processes and accuracy limitations, the prediction of the erosion prone area is limited to those areas with established beach profile monitoring programs and there also being some capacity to analyse data on an ongoing basis.

The final commonly used approach is the development of indices of vulnerability to erosion. This approach is most often used for hotspot assessments in the context of climate change adaptation. The benefits of this approach include its capacity to deal with a range of data availability and for the outcomes to inform risk management-based approaches. The main limitation of this approach is that it provides insufficient detail for addressing localised erosion issues, therefore requiring further assessments in order to quantify hazards adequately enough to determine necessary building setbacks and adaptation planning strategies.

1.2. Rethinking risk assessment approach

The prediction of SLR impacts on coastal areas is crucial for long-term coastal zone management and policy development. However, the task of strategy development and implementation is difficult due to uncertainties in the prediction of the spatial and temporal variability of these impacts (e.g. wave height, tide range, cyclonic events, coastal geomorphology, ecosystem types and land-use). Although uncertainty surrounding future climate change projection for small islands makes the impact assessments more difficult, this is not a good enough excuse for postponing or neglecting adaptation planning (Nurse et al., 2014). Most coastal adaptation planning options require long-term strategies addressing various aspects such as infrastructure, land use planning and flood protections (Wong et al., 2014). Therefore, suitable approaches must encapsulate uncertainty effectively through a range of scenarios should be considered for long-term adaptation planning.

As reported in a study (Gutierrez et al., 2011), a range of qualitative and quantitative methods were used to assess the impacts of SLR on shoreline change, which include: a bathtub approach that provides simple vulnerability prediction (McGranahan et al., 2007) but not addressing uncertainty (Gesch, 2009); and quantitative coastal erosion assessment (Gornitz et al., 2001) based on Bruun rules (Rosen, 1978). However, many of these methods fail to specifically address the considerable uncertainty involved in quantifying how factors influence the shoreline (Gutierrez et al., 2011). In previous studies, Gutierrez et al. (2011) developed a Bayesian Network (BN) model to demonstrate the probability of shoreline change rate on the U.S. Atlantic coast, while Dlamini (2011) developed a spatially explicit BN model to assess climate change impact on vegetation in Swaziland.

Following the suggested future research directions provided in these two previous studies, we coupled GIS and BN to generate probabilistic risk maps for predictions of coastal erosion in a small Pacific island, namely, Tanna Island, Vanuatu.

The integration of BN with GIS to generate probabilistic prediction maps for remote areas where data and maps are too limited to conduct traditional assessments is not prevalent in the literature. The novelty of the herein described and demonstrated approach is threefold: (a) the use of high-resolution raster datasets enables the authors to capture the variations along the coastline (10 m) for more accurate prediction; (b) development of a BN learned (structure and parameters) from data rather than using expert knowledge; and (c) rapid and interactive demonstration of probabilistic predictions through BN and GIS coupling, which is much less data and modelling intensive than detailed traditional physical modelling approaches. The developed approach can be applied to a range of environmental management problems, where either physical data is unavailable or difficult to collect, assessment budgets are limited, or local conditions are challenging for physical data collection. Moreover, it provides a user-friendly and low-cost visual assessment of environmental conditions and risks for various scenarios that would aid decision makers to narrow down the scope of subsequent expensive detailed physical modelling assessments.

2. Approach

2.1. Spatial Bayesian Network approach

BNs are an interactive, fast and efficient tool for modelling that has been increasingly gaining popularity for modelling hazard, vulnerability and risk assessments of complex ecosystems and environmental systems under great uncertainty (Uusitalo, 2007). A BN, named after mathematician Thomas Bayes (1702–1761), graphically represents knowledge about a given system and calculates causal dependencies between parts of that system through probabilities (Pearl, 1986).

A BN consists of a qualitative part (a directed acyclic graph - DAG) and a quantitative part (parameters specifying the conditional probability of each node given its parents described in DAG). A conditional probability table (CPT) quantifies the strength of influence between child nodes (variable) and parent nodes (Knochenhauer et al., 2013). The qualitative or quantitative value represents a state of a node. Each node must have, at least, two states and must represent all values that the node can take (Cain, 2001).

Fig. 1 (a) illustrates causal relationships between parent nodes (A and C) and the child node (B) with arbitrarily selected discrete states. Fig. 1 (b) shows the CPT defining the conditional relationships between parent nodes and the child node. For instance, the probability that B will be in “Good and Bad”, given the states of A and C.

The principle behind BN relies on Bayes theorem, which describes how prior knowledge about variable *A* will be updated based on observed evidence of *B*, and can be expressed by the following equation:

$$P(A|B) = P(B|A)P(A)/P(B) \quad (1)$$

where P(A | B) is the probability of *A* given *B* (posterior probability), P(B | A) is the probability of *B* given *A* (prior probability), P(B) is the prior (marginal) probability of *B*, and P(A) is prior probability of *A* (Aitkenhead and Aalders, 2009).

BN has been applied to a range of fields for assessing complex systems under a range of scenarios. In the context of climate change adaptation and risk assessment, recent BN applications include: climate change adaptive capacity assessment (Richards et al., 2016), impacts of extreme events on water quality and health (Bertone et al., 2016), water resources management (Phan et al., 2016), climate change impact on malaria transmission (Onyango et al., 2016), climate change impacts on the whale watching industry (Meynecke et al., 2017), coastal vulnerability to rising sea level (Bulteau et al., 2015; Gutierrez et al., 2011), a biological community-level vulnerability assessment to

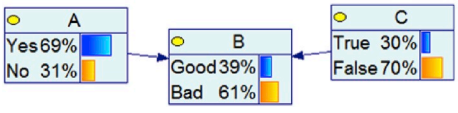

A	Yes		No	
C	True	False	True	False
Good	0.61	0.32	0.71	0.19
Bad	0.39	0.68	0.29	0.81

Fig. 1. A simple Bayesian Network and the conditional probability table.

changing climate(Hameed et al., 2013), ecosystem service assessment (Smith et al., 2018) and many other applications in the field of environmental management (Sperotto et al., 2017).

The spatial aspect of an environmental issue is crucial for stakeholders when making a decision as to where to implement their policies (Gonzalez-Redin et al., 2016). The spatial data processing tool GIS has the capability of storing, processing and visualising a range of data types (Sahin and Mohamed, 2013). Thus, GIS provides visualisation and spatial data processing capability for improving prediction accuracy by capturing spatial changes. Examples of GIS applications include: assessment of ecological vulnerability and potential impacts of natural, social, economic, environmental pollution, and human health (He et al., 2018), the assessment of a range of ecosystem services by utilising GIS and BN (Grêt-Regamey et al., 2013), and vulnerability assessment of physical and socio-economic impact of tropical cyclones on a coastal area (Sahoo and Bhaskaran, 2018). Considering the capability of both tools, some researchers have combined BN with GIS to generate probabilistic risk maps and help to improve shared understanding of stakeholders when dealing with spatially explicit issues. For example, mapping habitat suitability for endangered mammals (Smith et al., 2007), incorporating spatial GIS data and modelling spatial processes using spatial BN (Chee et al., 2016), mapping the abundance of riverine fish populations by combining GIS and BN (Wyatt, 2003), prediction of land cover changes (Aitkenhead and Aalders, 2009), prediction of long-term shoreline changes (Gutierrez et al., 2011), and deforestation (Mayfield et al., 2017).

Given the arguments presented above, we coupled BN with GIS in order to predict shoreline change by using spatial (raster layers) and non-spatial data obtained through fieldwork and stakeholder consultation, as detailed in the following section.

2.2. Case study area

Tanna Island of Vanuatu is a volcanic island located approx. 1750 km to the east of Australia, between New Caledonia and Fiji and covers an area of about 550 km^2. One of the areas with the lowest elevation is located within Port Resolution Bay, where there is a small village situated on an area with a higher elevation between Zone 10 and 12 (Fig. 2).

Port Resolution (Fig. 2) is a shallow bay located on the east of Tanna Island (Brothelande et al., 2015). Observed wave energy within the area is low, which can be attributed to the rocky headlands surrounding the bay (Kosciuch et al., 2018). The study area is divided into six main zone clusters according to their physical characteristics and then subdivided into 13 zones due to their exposure to wave and wind impacts as summarised in Fig. 2 and Table 1. A brief description of each of the six zone clusters is provided as follows:

- Zone cluster A (Zones 1 and 2): These two zones are surrounded by fringing reef and are directly impacted by North-easterly swell.
- Zone cluster B (Zones 3, 4 and 5): These zones are mainly comprised of an 840 m long (15 m high) rock cliff, located on the west part of Port Resolution and exposed to North-easterly swell and wind.
- Zone cluster C (Zones 6 and 7): These two zones are the only parts in a low area in Port Resolution Bay. They are characterised by a low lying beach in the Southern part of Port Resolution. The beach extends to around 1.3 km long and 10–40 m wide. The beach is characterised by a pronounced shore-parallel berm that has a maximum elevation of 1.8 m above MSL (Kosciuch et al., 2018). The landward side of the beach is vegetated with coconut trees and grass. The beach in Zone 7 has irregular topography caused by the presence of a river connected to the lake Eweya (Kosciuch et al., 2018).
- Zone cluster D (Zone 8, 9 and 10): These zones have a very narrow beach, or no beach surrounded by a 20 m cliff.
- Zone cluster E (Zone 11): This is quite a distinct zone on the North-eastern side of Port Resolution and mainly consists of two beaches separated by a rocky headland of 70 m wide and 100 m long. The two beaches dimensions are approximately 400 m long (10–30 m wide) and 200 m long (15–55 m wide), respectively. Seaward both beaches are surrounded by a fringing reef and landward of the beach is a vegetated area characterised by high-density coconut trees.
- Zone cluster F (Zone 12 and 13): These zones are located on the eastern side of Port Resolution and are commonly called 'white sand' beach. This beach extends 1.7 km from the northward to the southward of the east side of Port Resolution, and it is a 20–30 m wide beach. This beach is surrounded by a fringing reef, and landward of the beach is vegetated by grass with some bungalows and coconut trees.

Relevant data has been gathered from local, state and federal agencies, as well as academic institutions. The compilation of this data set is integral to map the potential coastal changes due to sea-level rise accurately.

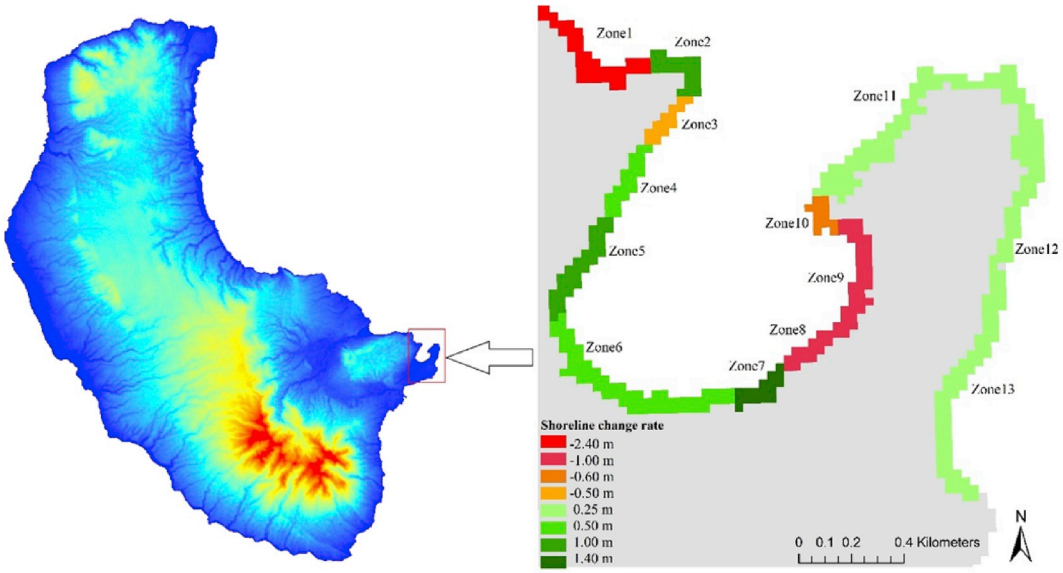

Fig. 2. Case study area and modelling zones: Port Resolution - Tanna Island, Vanuatu.

Table 1
Study area zone input data and physical characteristics used in BN.

Zones	Area (m^2)	Geomorphology	Coastal slope (%)	Mean wave height (m)	Max tidal range (m)	Relative sea level rise (mm/yr)	Presence of CR or artificial structures	Prior shoreline change (m/yr)
Zone 1	36,000	Beach, fringing reef	0.13	0.2–4	0.2–1.52	2–6	Yes	−2.4
Zone 2	18,900	Reef	0.18				Yes	1
Zone 3	12,600	Cliff, hard rock, no reef	5				No	N/A
Zone 4	18,900	Cliff, hard rock, no reef	5				No	N/A
Zone 5	28,800	Cliff, hard rock, no reef	5				No	N/A
Zone 6	57,600	Beach, no reef	0.04				No	0.5
Zone 7	15,300	Beach, no reef	0.08				No	1.4
Zone 8	19,800	Narrow beach, cliff	0.1				No	−1
Zone 9	27,000	Narrow beach, cliff	0.14				No	−1
Zone 10	10,800	Embayed beach, reef,	0.17				No	−0.6
Zone 11	66,600	Beach, fringing reef, headland	0.08				Yes	0.25
Zone 12	58,500	Open beach, fringing reef	0.12				Yes	0.25
Zone 13	60,300	Open beach, fringing reef	0.18				Yes	0.25

2.3. Bayesian Network (BN) development

In order to choose the best performing BN structure for predicting the shoreline change, three different BN models were built and tested using the Netica software package (Norsys, 2018): (1) a tree augmented network (TAN) (Fig. 3a); (2) a naive network (Fig. 3b); and (3) an Expert Structured Network (ESN) (Fig. 3c). For this process, 379 cases were used to learn three structures of seven nodes (Fig. 3). The Naive Bayes assumes that the target node (or class variable) is the only parent of all other nodes. The Naïve BN has very strong independence assumptions that, given the target node, all other variables are independent of each other (Doreswamy, 2011). TAN builds on the Naive Bayes structure by adding one more parent connection (in addition to the target node) between other variables in order to reflect dependencies between these nodes.

ESN involves experts and literature knowledge in constructing the BN. The TAN structure performed slightly better than ESN and Naive Bayes structures when evaluated with a prediction accuracy of 96%, compared to 94% and 92% respectively. Therefore, the TAN structure was used for GIS integration for predicting shoreline change (Fig. 4).

2.3.1. Key variables and data used in the BN

There are seven variables and relevant datasets obtained from a range of sources used in constructing the BN model (Table 1). Six predictor variables (i.e. Geomorphology (Gs), Coastal slope (Cs), Mean wave height (Wheight), Mean tidal range (Tr), Relative sea level rise (RSLR), Presence of coral reef or artificial structures (CR_exist)) were used to predict the probability of the target node (i.e. Shoreline change rate (SCRate)). Coastal slope and historical shoreline change for each zone have been calculated using Google Earth. Observed relative sea level between 1993 and 2010 in the southwest Pacific is higher than the global average of 3.3 mm/year (PRIF, 2017). Therefore, we have used five different RSLR figures ranging from 2 mm/yr to 6 mm/yr (PRIF, 2017). Wave height is relatively low (0.5–1.1 m) as the waves break on fringing reef crests and are highly sensitive to local bathymetry. The case study area is micro-tidal with of ~1.3 m. Based on the data obtained from a tide gauge installed at Port Resolution by our research team and the monthly sea level at Port Vila, Vanuatu from 1991 to 2018 (BOM, 2018), a tidal range between 0.2 and 1.6 m was used in the BN model.

Data for the location of coral reef and geomorphological characteristics of each zone was collected in the field. Finally, data for these seven variables was geocoded for use in spatial analysis. The data and/or method to determine the value of each of the variables listed in Table 1 is explained in the following sub-sections.

2.4. Data extraction methods

As mentioned previously, the selected probabilistic spatial BN approach developed for this study is much less data and modelling intensive than detailed physical modelling studies. Readily available data was utilised for populating the spatial BN model. Nonetheless, various data extraction techniques had to be used to sufficiently characterise the various coastal zones using best available data as described below.

2.4.1. Coastal slope estimation

The coastal slope was estimated either with in situ truth data collected in March 2017 or with Google Earth using data from SIO, NOAA, US Navy, NGA and GEBCO as shown in Fig. 5.

Coastal slope (%) that is assumed to be linear is calculated by using the following equation:

$$\text{Slope} = ((y_1 - y_2)/d) \quad (2)$$

where: y_1 = is the height of the vegetation line, y_2 = is the height of the waterline, and d = horizontal distance between y_1 and y_2 (as shown in Fig. 5).

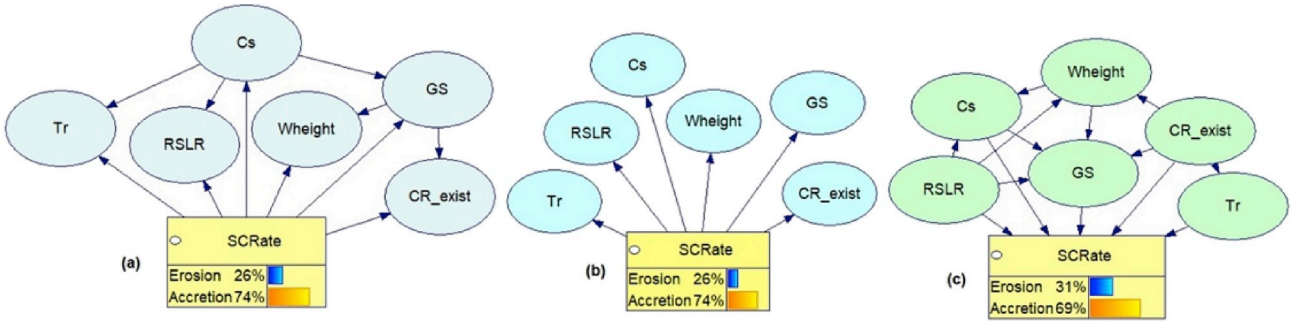

Fig. 3. Three BN structures: (a) TAN, (b) Naïve Network and (c) ESN adopted from Gutierrez et al. (Gutierrez et al., 2011).

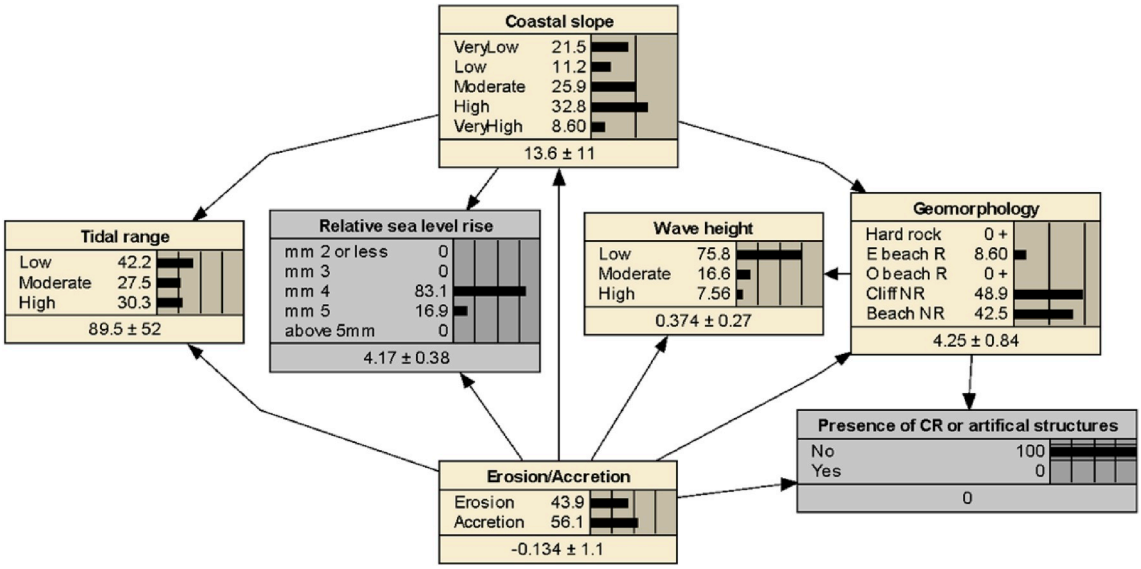

Fig. 4. TAN BN model for predicting the probability of shoreline change rate (erosion/accretion node in the figure) showing the result when the states of two nodes (the relative sea level rise and the presence of CR or artificial structures) was set to a particular scenario.

One of the limitations with the use of the Google Earth datasets, which is derived from a topography/bathymetry dataset (ETOPO), is the coarse resolution relative to the size of each of the zones. The resolution of the General Bathymetric Chart of the Oceans (GEBCO) data is around 1.8 km and 90 m for the topography. It is possible to sufficiently represent the slope despite the limited resolution. The highest point of the cliff was used as the ordinate and divided by the length of the slope.

2.4.2. Mean wave height estimation

Port Resolution is a shallow bay (i.e. −5 to -7 m above MSL), and the maximum wave set-up at the shoreline is estimated between 2.7 m and 3.85 m using Gourlay approximation (Gourlay, 1994).

No wave buoys are available for Port Resolution which made it difficult to verify the wave climate for this area. However regional wave hindcast models have been developed and are available for the Pacific islands. WAVEWATCH III (WWIII) is a third generation wave model developed at NOAA/NCEP in the spirit of the WAM model (Miles et al., 1995; The Wamdi Group, 1988). WWIII (Fig. 6 and Fig. 7) provides gridded and spectral waves from 1979 to present at the locations shown with the red dots ("aus.10 m") and orange dots ("Pac 4 m"). The average wave height is 1.7 m for the period from 2006 to 2016, and the mean direction is 118° (i.e. South-east direction).

Port Resolution is mainly exposed to South-easterly waves. Port Resolution is a pocket beach and waves arrive parallel to the shoreline, and longshore current are minimal, the wave energy within the bay is likely to be low due to the sheltering of the rocks/reef surrounding the bay. Wind force is found to be as decisive in driving pocket beach hydrodynamics, and the longshore current is mainly wind driven (Dehouck et al., 2009). Significant impacts will be associated with extreme events such as cyclones and tsunamis coming from the north direction. Gourlay (1994) reported the maximum sizes of waves on reef flats are controlled by water depth, and the maximum significant wave length (H_s) is approximately 0.55 times the water depth (d), including any wave-generated set-up (Gourlay, 1994; Kench and Brander, 2006). It is a challenge to predict wave climate for the remote islands with

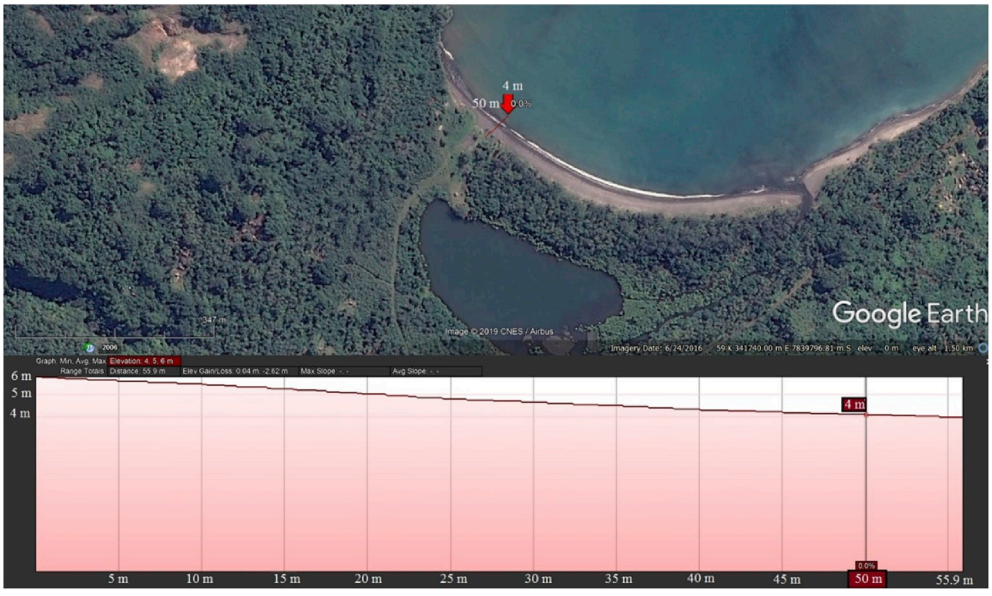

Fig. 5. Backshore beach profile in Zone 6 using Google Earth database (Source: GoogleEarth, 2019).

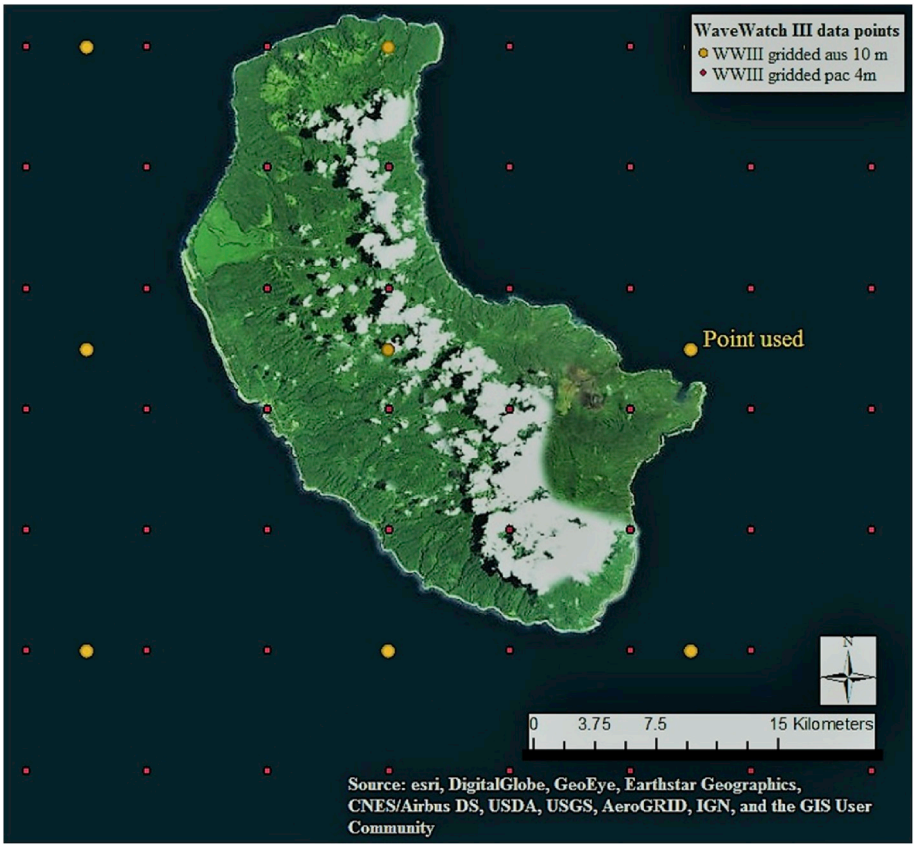

Fig. 6. WWIII wave data locations for Tanna Island.

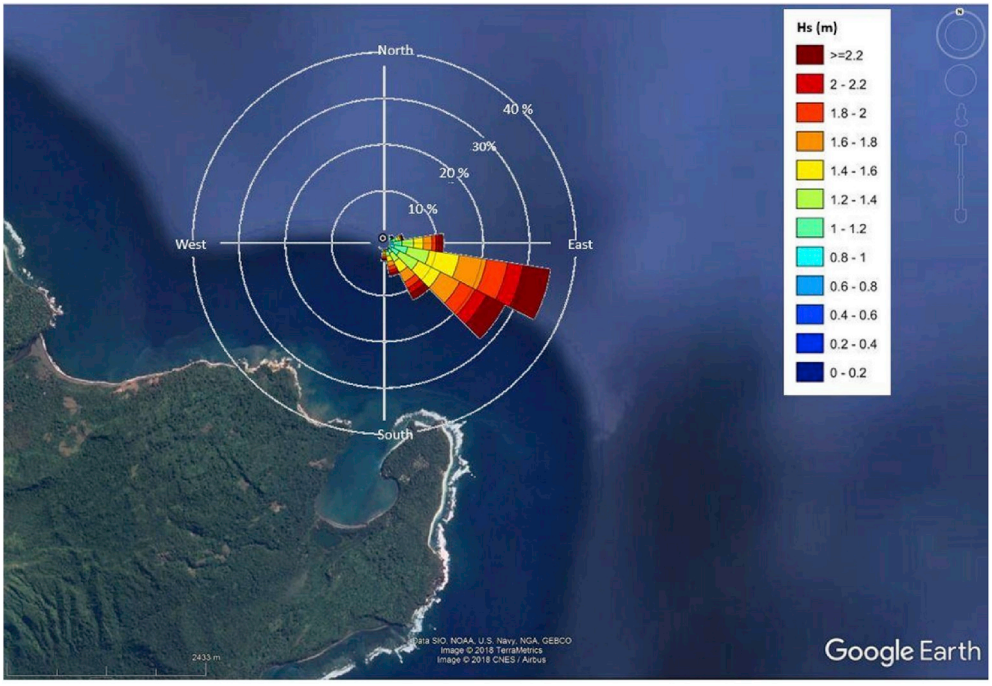

Fig. 7. Wave rose using WWIII gridded data from 2006 to 2016 (Lon: 169.5001; Lat: −19.4999).

limited or no data. To solve this issue, wave data (a timeseries of waves in the bay for a short period) was collected (Fig. 8). Data from WWIII and the wave buoy for this period have been compared and propagation from offshore to nearshore have been estimated from the data, observations during field trips and from interviews with local residents. The maximum wave run-up height found in the literature was less than 4 m during Tropical Cyclone Pam (TCP). In the study area, Port Resolution wave run-up has been estimated by Nishijima et al. (2015) during TCP as less than 4 m (Nishijima et al., 2015). This tropical cyclone is considered to be one of the worst experienced on Tanna Island

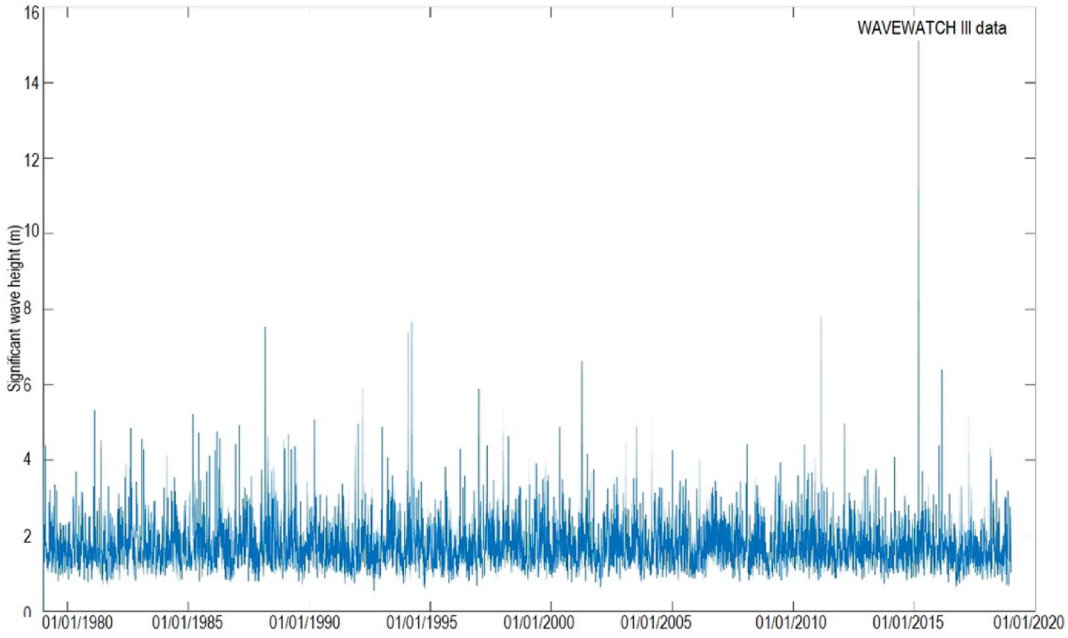

Fig. 8. Significant wave height using WAVEWATCH III (WWIII) data offshore for the period of 1979–2018.

and was considered a 100-year event. Accordingly, considering the offshore WWIII data, the collected wave data and interviews, the range of wave height for coastal impact in this study was determined as being between 0.2 and 4 m.

Fig. 8 shows hourly significant wave timeseries for the period of 1979–2018, which have been extracted from WWIII gridded wave data at the location of the point shown in Fig. 7 (Lon: 169.50,014°; lat: −19.499,939°). This point is located around 2 km from the entrance of the bay. Significant wave attenuation is expected due to the reef, the wave direction and local bathymetry.

2.4.3. Mean tidal range

Port Resolution Bay exhibits a micro-tidal range of ~1.3 m during the spring tide and ~0.4 m during neap tide. The mean sea level tide range used for this study was determined by tidal water levels collected by Griffith University at Port Resolution from the beginning of November 2016 to the end of March 2017. The lowest level of 0.2 m was during the neap tide in February (Date: 19/02/2017) and the highest tide level of 1.52 m was the maximum range during a spring tide in December (Date: 14/12/2017).

2.4.4. Relative sea level rise and prior shoreline change

The relative sea level range of 2–6 mm/year has been chosen based on historical records from the Pacific Sea Level Monitoring (PSLM) program that operates under the Climate and Oceans Support Program in the Pacific (COSPPac). The PSLM network is the only monitoring system of its kind in the Pacific. Shoreline change has been estimated with google earth using historical data from 2006 to 2016.

2.5. BN and GIS integration

BN provides the means to operationalise the conceptual system models. As illustrated in Fig. 9, the first step of BN and GIS integration is to define a BN structure to understand the coastal system qualitatively. The structure created using Netica software package (Norsys, 2018) (Figs. 3 and 4) shows the causal relationships between the system variables, where spatial data specific to the case study area was used. To populate the CPT for a node, the BN needs to be parameterised (Pollino et al., 2007). Prior to parameterisation, all seven nodes were categorised into states. The number of states assigned to each node was assigned on an individual basis (Fig. 4).

The input data used in the BN is based on GIS layers. Thus, as a second step, all datasets required to populate the BN input variables were converted to spatially explicit raster grids with a resolution of 10 m using ArcGIS (ESRI, 2014). Then, these spatial layers were converted to ASCII format to be read by GeoNetica software (Norsys, 2018).

The next step was to generate ASCII prediction maps using Netica for shoreline mobility. This step consists of analysing the most influential nodes affecting shoreline changes. In the last step, to export the data from the BN and back into a GIS, ASCII maps were converted to raster to create GIS prediction maps. These maps are resultant of the interactive probabilistic BN analysis by entering evidence within the BN.

3. Results and discussion

To understand how probabilities of the SLCR change when new information (evidence) is used to update the BN and resulting GIS maps, one of the essential interventions is to enter new evidence, which updates the probabilities to a new situation. Thus, the updated BN model presents the new posterior probability distribution representing the system's behaviour under the new evidence. In this way, the effect of changes in predictor variables on the target node examined whether the probability of SLRC is due to erosion or accretion.

Fig. 6 shows the Prior probability distributions for the BN nodes. The prior probabilities of accretion and erosion are induced by the evidence (prior probabilities of the input nodes) with 74.4% probability of Accretion and 25.6% Erosion.

Once the new evidence of RSLR for each category was entered, the impact was propagated through the network and, consequently, updating the probability distribution of target node (SLCR) which is probabilistically related to the evidence. The shoreline change graph (Fig. 10) shows that for RSLR categories above 4 mm/yr, the probabilities of erosion would increase to the highest level, 100%.

The shoreline change predictions computed by the BN generate an aggregated posterior probability for the entire case study area. Therefore, it is not clear whether this prediction applies to the whole coastline. While outside the scope of the present paper and word limit restrictions, the prediction should ideally be calculated for each

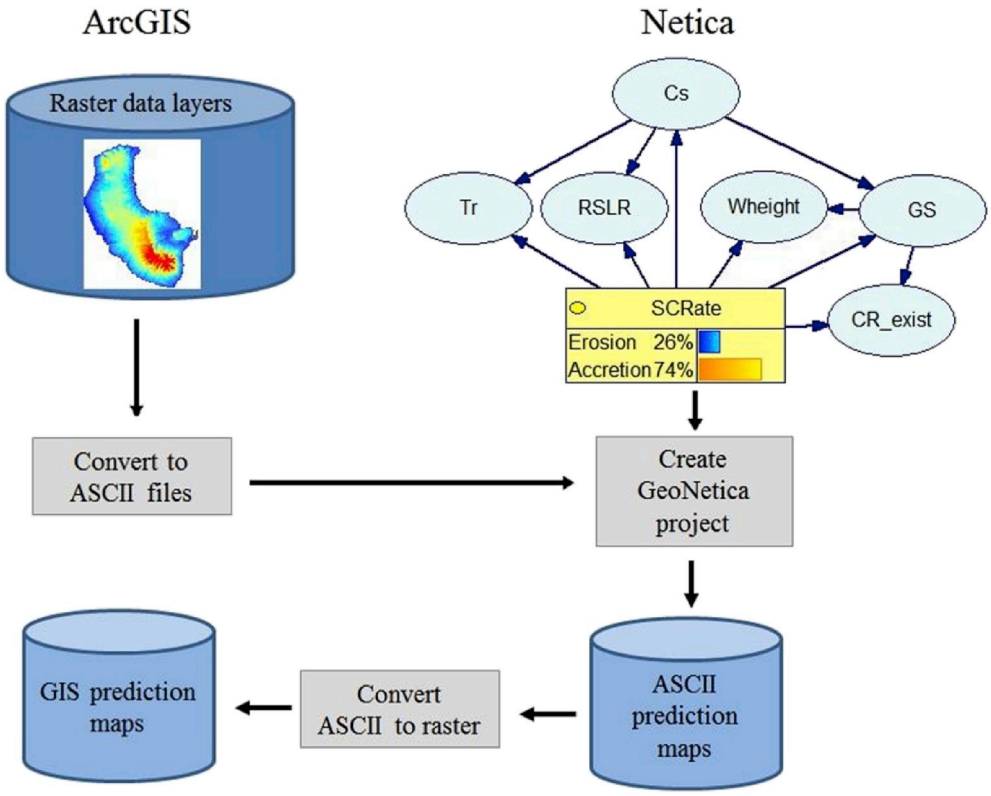

Fig. 9. Architecture for BN and GIS integration.

geographic location (i.e. zone) in order to better understand the localised impacts and to design specific adaptation management strategies for each zone cluster.

The use of BN alone is not enough to obtain spatial information for planning (Gonzalez-Redin et al., 2016). The integrated spatial BN addresses this limitation and provides spatial information to support planning and development decisions. As shown in Fig. 11, the spatial BN generates a spatially explicit prediction map for each of the states of the target node. The maps clearly show how erosion risks increase as the rising rates of sea level increase and provide invaluable information for the decision makers.

Fig. 12 shows the SLCR for each zone comparing the prior SLCR and the posterior SLCR for a RSLR scenario of above 4 mm/yr. The erosion rate is represented by negative values in red. Situations in Zone 4 and

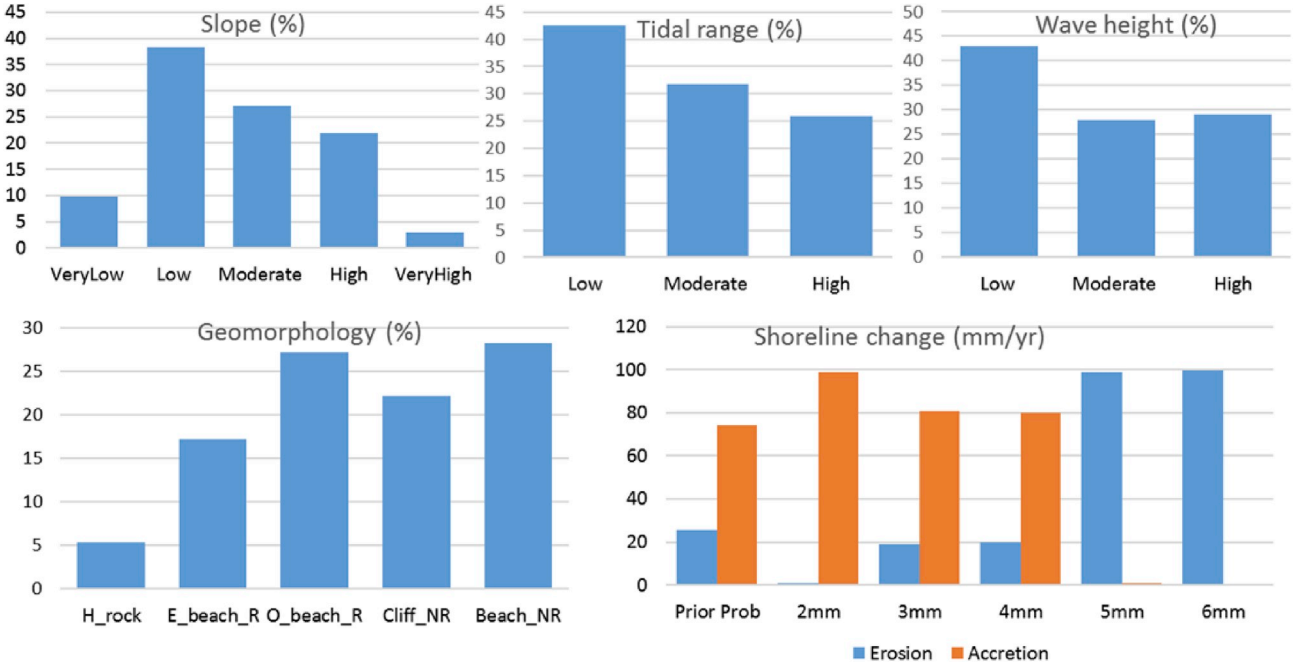

Fig. 10. Prior probability distributions for Geomorphology, Slope, Tidal range, and Wave height, nodes. The Shoreline change graph shows, in addition to the prior probability distribution, the posterior probability of Shoreline change rate for each RLSR rate category.

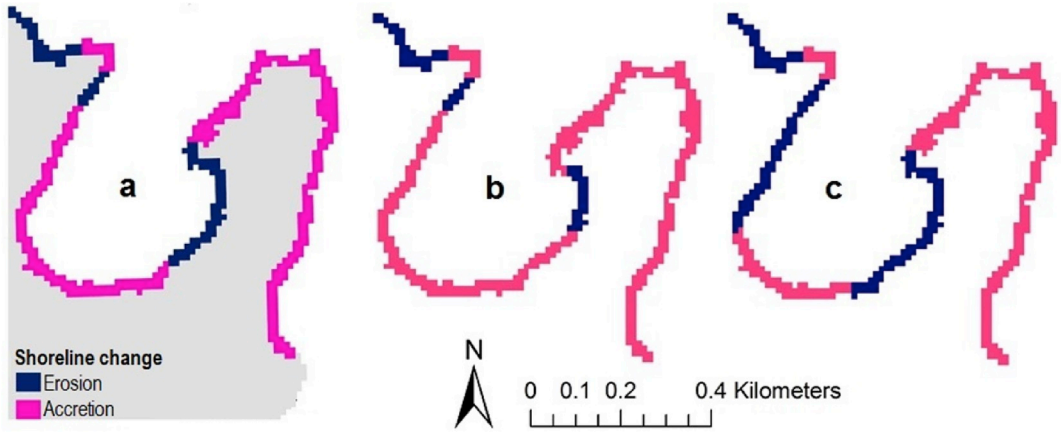

Fig. 11. Shoreline change prediction for Port Resolution, Tanna Island: a) RSLR = 3 mm/yr; b) RSLR ≤3 mm/yr; and c) RSLR ≥5 mm/yr.

Zone 5 change significantly from a stable condition (no significant erosion or accretion) to an erosion rate of 1.20 m/yr, respectively. Zone 1 maintains the most erosion-prone status. The erosion rates increase considerably in the other areas previously prone to erosion (Zone 3, Zone 8, Zone 9, and Zone 10).

3.1. Model evaluation

Performance evaluation is one of the critical elements of learning a BN structure. For this, we have conducted sensitivity and prediction performance metrics. The cross-validation method was utilised to evaluate the prediction performance of BN by using the same data set used for learning the BN model. In the cross-validation method, the dataset is divided into equally sized *k* sets (for our model, $k = 10$). Out of these *k* sets, one set is used for testing the remaining *k-1* sets. The training and testing process is repeated *k* times (Beuzen et al., 2017). Then, the overall performance of the BN is calculated by taking the average of the *k* folds. Resulting from the cross-validation exercise is the *Confusion Matrix* (Table 2), which shows the BN ability to predict both positive and negative shoreline change cases.

The BN model performance was evaluated using the standard metrics of accuracy and precision, which were calculated using the Confusion Matrix (Doreswamy, 2011). Accuracy (the proportion of the total number of predictions that were correct) and Precision (the rate of true positives out of all positive findings) was calculated using the following equations:

$$\text{Accuracy}(\%) = (TN + TP)/(TN + FN + FP + TP) \quad (3)$$

$$\text{Precision}(\%) = TP/(FP + TP) \quad (4)$$

where: TN (True Negative) shows the number of correct predictions; FP (False Positive) shows the number of incorrect predictions; FN (False Negative) represents the number of incorrect predictions, and TP (True Positive) shows the number of correct predictions.

Sensitivity analysis measures output variations due to changes in the input likelihood values. The degree of variation in a target node characterises the importance of input variables. For example, if the degree of change is big for a parameter, even a small change in this parameter leads to a significant variation in the posteriors of the target node. Thus, the higher the sensitivity, the more influential a parameter on the target node's posterior probability. This indicates the importance of the higher accuracy assessment of the parameter.

Sensitivity analysis was performed on the BN using the Netica software package (Table 3). The sensitivity analysis result shows that RSLR has the highest variance reduction followed by Cs and GS. This means that they are the most influential factors over the target node (SLCR). Variance reductions represent the expected reduction in variance of the value of SLCR (target variable) because of the finding at the varying nodes (predictors).

4. Conclusions and limitations

The prediction of future shoreline change is a challenging issue due

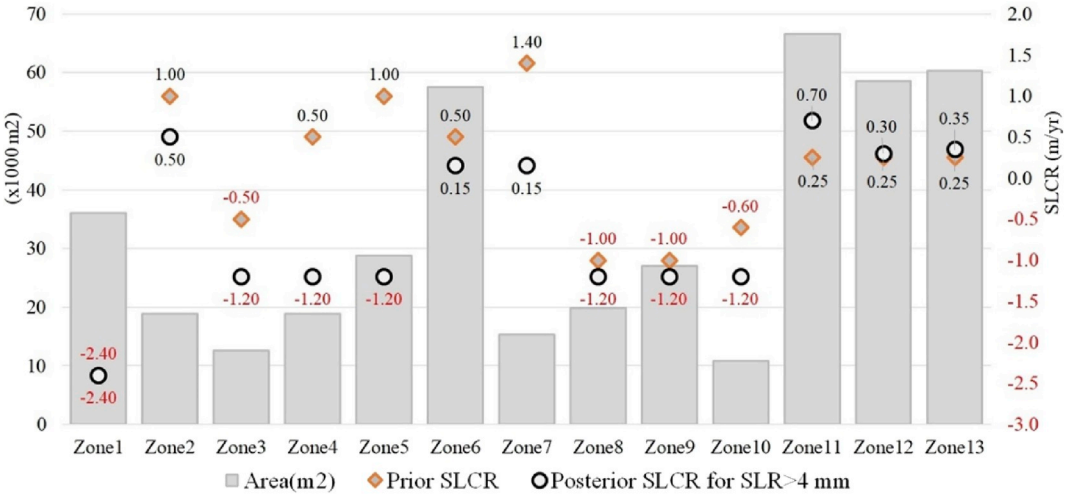

Fig. 12. Shoreline change rates for each geographic location. The primary ordinate (LHS) represents surface area (× 1000 m^2) and the secondary ordinate (SLCR) shows the shoreline change rate (m/yr).

Table 2
Confusion matrix.

Title here		Actual		
		Positive (Erosion)	Negative (Accretion)	Precision
Test	Positive (Erosion)	TN = 84	FP = 13	(84/97) = 0.865,979
	Negative (Accretion)	FN = 1	TP = 281	(281/282) = 0.996,454
	Overall sample	SCRate prediction accuracy		(365/379) = 0.963,061

Table 3
Results from sensitivity analysis (variance reduction analysis): Input variables and their effects on posterior outputs.

Variables	Type	Variance Reduction (%)
Relative sea level rise (RSLR) (mm/yr)	Discrete	36.7
Coastal slope (Cs) (%)	Continuous	21
Geomorphology (GS)	Discrete	17.1
Presence of CR or artificial structures	Discrete	4.06
Tidal range (Tr) (cm)	Continuous	2.22
Wave height (Wh) (m)	Continuous	0.122

to a range of complex factors contributing to inherent uncertainties and the absence of high-resolution data required for sophisticated physical modelling. The complexity requires integrated robust approaches to understand the causal relationships between the system components. The BN approach provides a robust platform for modelling the complex interactions of these factors influencing the shoreline changes and to quantify the prediction uncertainty. The proposed spatial BN, through the integration of BN with GIS, offers a new tool to generate probabilistic prediction maps of likely climate change related erosion impacts. As demonstrated by the performance evaluation of the model, the BN model achieved 96.3% accuracy in predicting the correct shoreline change, 365 out of 379 cases. The spatial BN offers instrumental insights for spatially explicit analysis of factors affecting shoreline mobility and can be used by decision makers to develop and prioritise effective management options.

Further work is necessary to determine how this type of vulnerability index approach can be used to inform decisions making. Moreover, the advantages, disadvantages and limitations of this approach, when compared to alternative approaches for climate change adaptation planning at the local scale, need to be examined. The approach may be developed to incorporate higher resolution data outputs from localised coastal process models; it can also augment planning outputs similar to those generated by erosion prone area and beach volume index approaches to coastal erosion hazard assessment. Coupled BN-GIS models have a wide range of applications for climate change adaptation planning. The probabilistic features of BN make it useful for conducting long-term risk assessments where there is a high degree of uncertainty with the scenario input parameters, and GIS allows decision-makers to instantly visualise the impacts of various scenarios at various scales (i.e. local, regional, and country). Water and food security, land use, bio-diversity, flooding, to name a few, are all climate change related issues that could be assessed using a spatial BN approach. The efficiency of this approach (i.e. not data, human resourced, or modelling intensive) makes it ideal for preliminary vulnerability assessments in order to identify those areas prone to significant climate change impacts, so that resource intensive in-depth scientific and engineering studies can be targeted on those critical areas.

Besides, with an increasing spatial resolution of observations, the problem of data complexity becomes significant. The algorithmic complexity of the environmental setting itself has to be evaluated (Papadimitriou, 2009, 2012), which, in turn, is the source of the ensuing computational complexity in handling the models and simulations that describe that environmental setting. This increase in computational complexity has been documented for spatial Bayesian models also (Eidsvik et al., 2012; Ren et al., 2011) and this prompts for future research that would focus on discovering new “smart” methods for reducing the complexity of datasets of environmental geodata.

The attenuation of the wave over the reef is debatable. Further research needs to be done to estimate the dissipation of the wave over the reef and impacts to the coast. The reef geomorphology and water depth play a significant role in the waves' dissipation, and data collection is crucial for improvement in the method. A first pass using Google Earth gives a good approximation of the data, but the coarseness in resolution of this dataset means that it is insufficient for estimating the cliff erosion.

Acknowledgments

This research was supported by a grant from a Private Charitable Trust.

References

Aitkenhead, M.J., Aalders, I.H., 2009. Predicting land cover using GIS, Bayesian and evolutionary algorithm methods. J. Environ. Manag. 90, 236–250.
Alexandrakis, G., Poulos, S.E., 2014. An holistic approach to beach erosion vulnerability assessment. Sci Rep-Uk 4.
Bertone, E., Sahin, O., Richards, R., Roiko, A., 2016. Extreme events, water quality and health: a participatory Bayesian risk assessment tool for managers of reservoirs. J. Clean. Prod. 135, 657–667.
Beuzen, T., Splinter, K.D., Turner, I.L., Harley, M.D., Marshall, L., 2017. In: Predicting Storm Erosion on Sandy Coastlines Using a Bayesian Network, Coasts & Ports 2017 Conference – Cairns, 21-23 June 2017.
BOM, 2018. Monthly Sea Levels for VANUATU. Bureau of Meteorology Available: http://www.bom.gov.au/ntc/IDO70059/IDO70059SLI.shtml.
Brothelande, E., Lénat, J.F., Normier, A., Bacri, C., Peltier, A., Paris, R., Kelfoun, K., Merle, O., Finizola, A., Garaebiti, E., 2015. Insights into the evolution of the Yenkahe resurgent dome (Siwi caldera, Tanna Island, Vanuatu) inferred from aerial high-resolution photogrammetry. J. Volcanol. Geotherm. Res. 299, 78.
Bulteau, T., Baills, A., Petitjean, L., Garcin, M., Palanisamy, H., Le Cozannet, G., 2015. Gaining insight into regional coastal changes on La Reunion island through a Bayesian data mining approach. Geomorphology 228, 134–146.
Cain, J.D., 2001. Planning Improvements in Natural Resources Management: Guidelines for Using Bayesian Networks to Support the Planning and Management of Development Programmes in the Water Sector and beyond. Centre for Ecology and Hydrology.
Chee, Y.E., Wilkinson, L., Nicholson, A.E., Quintana-Ascencio, P.F., Fauth, J.E., Hall, D., Ponzio, K.J., Rumpff, L., 2016. Modelling spatial and temporal changes with GIS and spatial and dynamic Bayesian Networks. Environ. Model. Softw 82, 108–120.
Dehouck, A., Dupuis, H., Senechal, N., 2009. Pocket beach hydrodynamics: the example of four macrotidal beaches, Brittany, France. Mar. Geol. 266, 1–17.
Dlamini, W., 2011. Probabilistic spatio-temporal assessment of vegetation vulnerability to climate change in Swaziland. Glob. Chang. Biol. 17, 1425–1441.
Doreswamy, H.K.S., 2011. Performance evaluation of predictive classifiers for knowledge discovery from engineering materials data sets. CIIT International Journal of Artificial Intelligent Systems and Machine Learning 3, 162–168.
Eidsvik, J., Finley, A.O., Banerjee, S., Rue, H., 2012. Approximate Bayesian inference for large spatial datasets using predictive process models. Comput. Stat. Data Anal. 56, 1362–1380.
ESRI, 2014. ArcGIS Desktop: Release 10.3. Environmental Systems Research Institute, Redlands, CA.
Gesch, D.B., 2009. Analysis of lidar elevation data for improved identification and delineation of lands vulnerable to sea-level rise. J. Coast. Res. 49–58.
Gonzalez-Redin, J., Luque, S., Poggio, L., Smith, R., Gimona, A., 2016. Spatial Bayesian belief networks as a planning decision tool for mapping ecosystem services trade-offs on forested landscapes. Environ. Res. 144, 15–26.
GoogleEarth, 2019. Pro V 7.3.2.5491 (June 24, 2016). Port Resolution, Tanna Island, Vanuatu 59 K 341740.00m E 7839796.81 M S Elevation 0 M, Eye Alt 1.50 Km. Image CNES/Airbus 2019.
Gornitz, V., Couch, S., Hartig, E.K., 2001. Impacts of sea level rise in the New York City

metropolitan area. Glob. Planet. Chang. 32, 61–88.
Gourlay, M.R., 1994. Wave transformation on a coral-reef. Coast Eng. 23, 17–42.
Grêt-Regamey, A., Brunner, S.H., Altwegg, J., Bebi, P., 2013. Facing uncertainty in ecosystem services-based resource management. J. Environ. Manag. 127, S145–S154.
Gutierrez, B.T., Plant, N.G., Thieler, E.R., 2011. A Bayesian Network to predict coastal vulnerability to sea level rise. J Geophys Res-Earth 116.
Hameed, S.O., Holzer, K.A., Doerr, A.N., Baty, J.H., Schwartz, M.W., 2013. The value of a multi-faceted climate change vulnerability assessment to managing protected lands: lessons from a case study in Point Reyes National Seashore. J. Environ. Manag. 121, 37–47.
He, L., Shen, J., Zhang, Y., 2018. Ecological vulnerability assessment for ecological conservation and environmental management. J. Environ. Manag. 206, 1115–1125.
Hewitson, B., Janetos, A.C., Carter, T.R., Giorgi, F., Jones, R.G., Kwon, W.-T., Mearns, L.O., Schipper, E.L.F., van Aalst, M., 2014. Regional context. In: Barros, V.R., Field, C.B., Dokken, D.J., Mastrandrea, M.D., Mach, K.J., Bilir, T.E., Chatterjee, M., Ebi, K.L., Estrada, Y.O., Genova, R.C., Girma, B., Kissel, E.S., Levy, A.N., MacCracken, S., Mastrandrea, P.R., White, L.L. (Eds.), Climate Change 2014: Impacts, Adaptation, and Vulnerability. Part B: Regional Aspects. Contribution of Working Group II to the Fifth Assessment Report of the Intergovernmental Panel on Climate Change. Cambridge University Press, Cambridge, United Kingdom and New York, NY, USA, pp. 1133–1197.
Kench, P.S., Brander, R.W., 2006. Wave processes on coral reef flats: implications for reef geomorphology using Australian case studies. J. Coast. Res. 22, 209–223.
Knochenhauer, M., Swaling, V.H., Dedda, F.D., Hansson, F., Sjoekvist, S., Sunnegaerd, K., 2013. Using Bayesian Belief Network (BBN) Modelling for Rapid Source Term Prediction Final Report (NKS–293). Denmark.
Kosciuch, T.J., Pilarczyk, J.E., Hong, I., Fritz, H.M., Horton, B.P., Rarai, A., Harrison, M.J., Jockley, F.R., 2018. Foraminifera reveal a shallow nearshore origin for overwash sediments deposited by Tropical Cyclone Pam in Vanuatu (South Pacific). Mar. Geol. 396, 171–185.
Mayfield, H., Smith, C., Gallagher, M., Hockings, M., 2017. Use of freely available datasets and machine learning methods in predicting deforestation. Environ. Model. Softw 87, 17–28.
McGranahan, G., Balk, D., Anderson, B., 2007. The rising tide: assessing the risks of climate change and human settlements in low elevation coastal zones. Environ. Urbanization 19, 17–37.
Meynecke, J.O., Richards, R., Sahin, O., 2017. Whale watch or no watch: the Australian whale watching tourism industry and climate change. Reg. Environ. Change 17, 477–488.
Miles, J., Gj, Cavaleri, L., Donelan, M., Hasselmann, K., Hasselmann, S., Janssen, Paem, 1995. Dynamics and modeling of ocean waves - komen. Science 270 320-320.
Nishijima, K., Mori, N., Yasuda, T., Shimura, T., 2015. DPRI-VMGD Joint Survey for Cyclone Pam Damages. Vanuatu Meteorology and Geo-Hazard Department, Port-Vila, Vanuatu [online] available at: http://www.taifu.dpri.kyoto-u.ac.jp/wp-content/uploads/2015/05/DPRI-VMGD-survey-first-report-Final.pdf, Accessed date: 20 October 2018.
Norsys, 2018. Netica - Bayesian Network Software. Norsys Software Corp, Vancouver, Canada Available: http://www.norsys.com/.
Nurse, L.A., McLean, R.F., Agard, J., Briguglio, L.P., Duvat-Magnan, V., Pelesikoti, N., Tompkins, E., Webb, A., 2014. Small islands. In: Barros, V.R., Field, C.B., Dokken, D.J., Mastrandrea, M.D., Mach, K.J., Bilir, T.E., Chatterjee, M., Ebi, K.L., Estrada, Y.O., Genova, R.C., Girma, B., Kissel, E.S., Levy, A.N., MacCracken, S., Mastrandrea, P.R., White, L.L. (Eds.), Climate Change 2014: Impacts, Adaptation, and Vulnerability. Part B: Regional Aspects. Contribution of Working Group II to the Fifth Assessment Report of the Intergovernmental Panel on Climate Change. Cambridge University Press Cambridge, United Kingdom and New York, NY, USA, pp. 1613–1654.
Onyango, E.A., Sahin, O., Awiti, A., Chu, C., Mackey, B., 2016. An integrated risk and vulnerability assessment framework for climate change and malaria transmission in East Africa. Malar. J. 15, 551.
Papadimitriou, F., 2009. Modelling spatial landscape complexity using the Levenshtein algorithm. Ecol. Inf. 4, 48–55.
Papadimitriou, F., 2012. The algorithmic complexity of landscapes. Landsc. Res. 37, 591–611.
Pearl, J., 1986. Fusion, propagation, and structuring in belief networks. Artif. Intell. 29, 241–288.
Phan, T.D., Smart, J.C.R., Capon, S.J., Hadwen, W.L., Sahin, O., 2016. Applications of Bayesian belief networks in water resource management: a systematic review. Environ. Model. Softw 85, 98–111.
Pollino, C.A., Woodberry, O., Nicholson, A., Korb, K., Hart, B.T., 2007. Parameterisation and evaluation of a Bayesian Network for use in an ecological risk assessment. Environ. Model. Softw 22, 1140–1152.
PRIF, 2017. Guidance for Coastal Protection Works in Pacific Island Countries, 2017. Design Guidance Report. Pacific Region Infrastructure Facility, Sydney, New South Wales, Australia Available: www.theprif.org.
Ren, Q., Banerjee, S., Finley, A.O., Hodges, J.S., 2011. Variational Bayesian methods for spatial data analysis. Comput. Stat. Data Anal. 55, 3197–3217.
Richards, R.G., Sano, M., Sahin, O., 2016. Exploring climate change adaptive capacity of surf life saving in Australia using Bayesian belief networks. Ocean Coast Manag. 120, 148–159.
Rosen, P.S., 1978. A regional test of the Bruun Rule on shoreline erosion. Mar. Geol. 26, M7–M16.
Sahin, O., Mohamed, S., 2013. A spatial temporal decision framework for adaptation to sea level rise. Environ. Model. Softw 46, 129–141.
Sahoo, B., Bhaskaran, P.K., 2018. Multi-hazard risk assessment of coastal vulnerability from tropical cyclones – a GIS based approach for the Odisha coast. J. Environ. Manag. 206, 1166–1178.
Shand, T., Reinen-Hamill, R., Kench, P., Ivamy, M., Knook, P., Howse, B., 2015. Methods for probabilistic coastal erosion hazard assessment [online]. 2015 In: Australasian Coasts & Ports Conference: 22nd Australasian Coastal and Ocean Engineering Conference and the 15th Australasian Port and Harbour Conference. Engineers Australia and IPENZ, Auckland, New Zealand, pp. 814–820. Availability: https://search-informit-com-au.libraryproxy.griffith.edu.au/documentSummary;dn=725013041606632;res=IELENG ISBN:%209781922107794.
Smith, C.S., Howes, A.L., Price, B., McAlpine, C.A., 2007. Using a Bayesian belief network to predict suitable habitat of an endangered mammal – the Julia Creek dunnart (Sminthopsis douglasi). Biol. Conserv. 139, 333–347.
Smith, R.I., Barton, D.N., Dick, J., Haines-Young, R., Madsen, A.L., Rusch, G.M., Termansen, M., Woods, H., Carvalho, L., Giucă, R.C., Luque, S., Odee, D., Rusch, V., Saarikoski, H., Adamescu, C.M., Dunford, R., Ochieng, J., Gonzalez-Redin, J., Stange, E., Vădineanu, A., Verweij, P., Vikström, S., 2018. Operationalising ecosystem service assessment in bayesian belief networks: experiences within the OpenNESS project. Ecosystem Services 29, 452–464.
Sperotto, A., Molina, J.-L., Torresan, S., Critto, A., Marcomini, A., 2017. Reviewing Bayesian Networks potentials for climate change impacts assessment and management: a multi-risk perspective. J. Environ. Manag. 202, 320–331.
The Wamdi Group, 1988. The WAM model—a third generation ocean wave prediction model. J. Phys. Oceanogr. 18, 1775–1810.
Todd, D., Strauss, D., Murray, T., Tomlinson, R., Hunt, S., Bowra, K., 2015. Beach volume index: management tool for the Gold Coast beaches [online]. 2015 In: Australasian Coasts & Ports Conference 2015: 22nd Australasian Coastal and Ocean Engineering Conference and the 15th Australasian Port and Harbour Conference. Engineers Australia and IPENZ, Auckland, New Zealand, pp. 906–912. Availability: https://search.informit.com.au/documentSummary;dn=725516131830603;res=IELENG ISBN:%209781922107794.
Uusitalo, L., 2007. Advantages and challenges of Bayesian Networks in environmental modelling. Ecol. Model. 203, 312–318.
Wong, P.P., Losada, I.J., Gattuso, J.-P., Hinkel, J., Khattabi, A., McInnes, K.L., Saito, Y., Sallenger, A., 2014. Coastal systems and low-lying areas. In: Field, C.B., Barros, V.R., Dokken, D.J., Mach, K.J., Mastrandrea, M.D., Bilir, T.E., Chatterjee, M., Ebi, K.L., Estrada, Y.O., Genova, R.C., Girma, B., Kissel, E.S., Levy, A.N., MacCracken, S., Mastrandrea, P.R., White, L.L. (Eds.), Climate Change 2014: Impacts,Adaptation, and Vulnerability. Part A: Global and Sectoral Aspects. Contribution of Working Group II to the Fifth Assessment Report of the Intergovernmental Panel on Climate Change. Cambridge University Press, Cambridge, United Kingdom and New York, NY, USA, pp. 361–409.
Wyatt, R.J., 2003. Mapping the abundance of riverine fish populations: integrating hierarchical Bayesian models with a geographic information system (GIS). Can. J. Fish. Aquat. Sci. 60, 997–1006.